2-Acetylpyridine Thiosemicarbazones are Potent Iron Chelators and Antiproliferative Agents: Redox Activity, Iron Complexation and Characterization of their Antitumor Activity

Des R. Richardson,*[,†] Danuta S. Kalinowski,[†] Vera Richardson,[†] Philip C. Sharpe,[‡] David B. Lovejoy,[†] Mohammad Islam,[‡] and Paul V. Bernhardt*[,‡]

Department of Pathology and Bosch Institute, University of Sydney, Sydney, New South Wales 2006, Australia, Centre for Metals in Biology, School of Chemistry and Molecular Biosciences, University of Queensland, Brisbane, Queensland 4072, Australia

Received December 15, 2008

Through systematic structure−activity studies of the 2-benzoylpyridine thiosemicarbazone (HBpT), 2-(3-nitrobenzoyl)pyridine thiosemicarbazone (HNBpT) and dipyridylketone thiosemicarbazone (HDpT) series of iron (Fe) chelators, we identified structural features necessary to form Fe complexes with potent anticancer activity (*J. Med. Chem.* **2007**, *50*, 3716−3729). In this investigation, we generated the related 2-acetylpyridine thiosemicarbazone (HApT) analogues to examine the influence of the methyl group at the imine carbon. Four of the six HApT chelators had potent antitumor activity (IC_{50}: 0.001−0.002 μM) and Fe chelation efficacy that was similar to the most effective HBpT and HDpT ligands. The HApT Fe complexes had the lowest $Fe^{III/II}$ redox potentials of any thiosemicarbazone series we have generated. This property, in combination with their ability to effectively chelate cellular Fe, make the HApT series one of the most potent antiproliferative agents developed by our group.

Introduction

Iron (Fe) chelators were originally designed for the treatment of iron overload disease.[1−3] However, more recently, a number of studies have demonstrated that Fe chelators are an emerging class of agents that show effective antitumor activity in vitro and in vivo and can overcome resistance to standard chemotherapy.[4−10] In fact, the ability of chelators to overcome resistance and inhibit tumor growth probably relates to their ability to affect multiple molecular targets.[11] These include the enzyme responsible for the rate-limiting step of DNA synthesis, ribonucleotide reductase,[1,11−14] and molecules involved in cell cycle control (e.g., cyclin D1, $p21^{CIP1/WAF1}$)[15−17] and the inhibition of metastasis (i.e., *N-myc downstream regulated gene-1*).[18]

Initial interest in the development of chelators for cancer treatment began with desferrioxamine (DFO[a]; Figure 1), the "gold-standard" therapeutic for the treatment of iron overload disease.[1,2] However, DFO suffers numerous problems, including low membrane permeability and short plasma half-life and thus this drug needs to be subcutaneously infused for long periods (12−24 h/day, 5−6 days/week).[2] Chelators such as DFO inhibit tumor growth, at least in part, by inducing whole body Fe-depletion.[1] Therefore, this is not an appropriate approach in the treatment of cancer, as many patients suffer the anemia of chronic disease. Thus, whole body Fe depletion would not be appropriate.

More recently, investigations from our laboratories have led to the development of the dipyridylketone thiosemicarbazone (HDpT; Figure 1) class of chelators that demonstrate potent and selective antitumor activity in vitro and in vivo.[5,7,19,20] Studies using mouse and human tumor xenograft models have shown that dipyridylketone 4,4-dimethyl-3-thiosemicarbazone (HDp44mT; 0.4−0.75 mg/kg) markedly inhibits tumor growth but does not induce whole body Fe depletion at these doses.[20] The mechanism of action of these compounds in vivo appears to be due to the formation of an intracellular redox-active Fe complex in tumors that generates cytotoxic reactive oxygen species.[5,19]

Further assessment of the HDpT analogues led to the examination of the role of aromatic substituents on the antiproliferative and redox activity of novel HDpT analogues, namely the 2-benzoylpyridine thiosemicarbazone (HBpT) and 2-(3-nitrobenzoyl)pyridine thiosemicarbazone (HNBpT) analogues[7] (Figure 1). These latter ligands possess the same set of (N,N,S) donor atoms as the HDpT analogues, but have different noncoordinating substituents.[7] Like the HDpT chelators, they typically form 2:1 ligand:metal complexes with six-coordinate metal ions. Both series exhibited selective antiproliferative effects, with the majority having greater antineoplastic activity than their HDpT homologues.[7] This made the HBpT chelators the most active anticancer agents developed in our laboratory.[7]

The HBpT series Fe complexes exhibited lower redox potentials than their corresponding HDpT and HNBpT complexes, highlighting their enhanced redox activity.[7] The increased ability of BpT−Fe complexes to catalyze ascorbate oxidation and benzoate hydroxylation, relative to their HDpT and HNBpT analogues, suggested that redox cycling played an important role in their antiproliferative activity.[7] It is significant to note that redox cycling of the metal complex is only one

* To whom correspondence should be addressed. For D.R.R.: phone, +61-2-9036-6548; fax, +61-2-9351-3429; E-mail, d.richardson@med.usyd.edu.au. For P.V.B.: phone, +61-7-3365-4266; fax, +61-7-3365-4299; E-mail, p.bernhardt@uq.edu.au.

† Department of Pathology and Bosch Institute, University of Sydney.

‡ Centre for Metals in Biology, School of Chemistry and Molecular Biosciences, University of Queensland.

[a] Abbreviations: 3-AP, 3-aminopyridinecarbaldehyde thiosemicarbazone; DFO, desferrioxamine B; DMF, dimethyl formamide; Fe_2-Tf, diferric transferrin; HAPBH, 2-acetylpyridine benzoyl hydrazone; HApT, 2-acetylpyridine thiosemicarbazone; HAp4aT, 2-acetylpyridine 4-allyl-3-thiosemicarbazone; HAp4eT, 2-acetylpyridine 4-ethyl-3-thiosemicarbazone; HAp4mT, 2-acetylpyridine 4-methyl-3-thiosemicarbazone; HAp44mT, 2-acetylpyridine 4,4-dimethyl-3-thiosemicarbazone; HAp4pT, 2-acetylpyridine 4-phenyl-3-thiosemicarbazone; HBPBH, 2-benzoylpyridine benzoyl hydrazone; HBpT, 2-benzoylpyridine thiosemicarbazone; HBp4eT, 2-benzoylpyridine 4-ethyl-3-thiosemicarbazone; HDpT, dipyridylketone thiosemicarbazone; HDp44mT, dipyridylketone 4,4-dimethyl-3-thiosemicarbazone; HNBpT, 2-(3-nitrobenzoyl)pyridine thiosemicarbazone; H_2NIH/311, 2-hydroxy-1-naphthaldehyde isonicotinoyl hydrazone; H_2PIH, pyridoxal isonicotinoyl hydrazone; HPKBH, dipyridylketone isonicotinoyl hydrazone; IBE, iron-binding equivalent; L1, deferiprone; MeCN, acetonitrile; MLCT, metal to ligand charge transfer; NHE, normal hydrogen electrode; RR, ribonucleotide reductase.

10.1021/jm801585u CCC: $40.75
Published on Web 02/13/2009

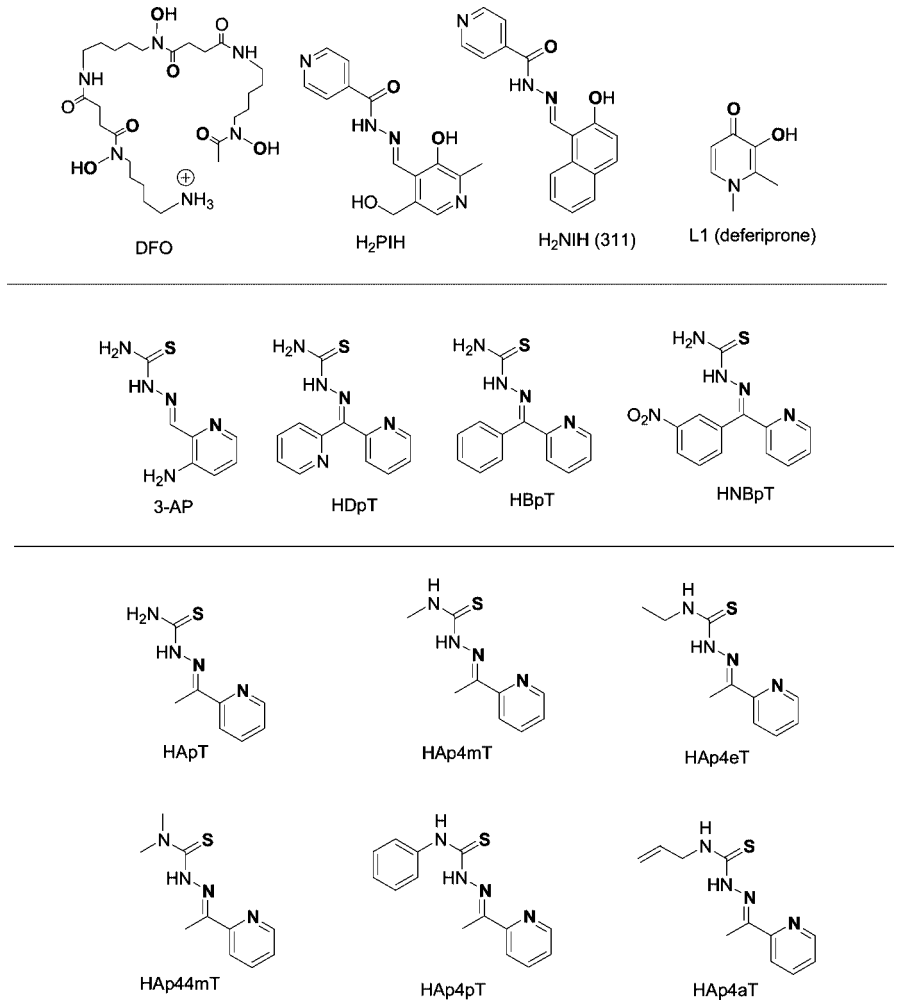

Figure 1. Line drawings of existing and novel Fe chelators discussed herein.

mechanism by which these chelators induce antiproliferative activity. In fact, other ligands such as 2-hydroxy-1-naphthylaldehyde isonicotinoyl hydrazone (311) induce their antiproliferative effects via Fe depletion and this is also an effect of the HDpT and HNBpT analogues.[1,5,6,19]

Thiosemicarbazones have a long history and broad spectrum of biological efficacy[21−26] that includes antimalarial,[27−29] antimicrobial,[30−35] and antitumor activity.[36−47] However, the link between the biological activity of thiosemicarbazones and their Fe coordination chemistry has only emerged more recently and we have focused on this particular aspect.[5,7,19] The thiosemicarbazone that has attracted most attention is 3-aminopyridinecarbaldehyde thiosemicarbazone (3-AP; Figure 1), which is currently undergoing phase II trials for the treatment of a range of cancers.[48−54]

Considering our results with the HDpT and HBpT analogues,[7] together with the fact that the structurally similar and clinically trialed thiosemicarbazone Fe chelator 3-AP[8,55] shows high antiproliferative activity, further studies were implemented to examine the effect of replacing the parent ketone of HDpT (di-2-pyridylketone) with 2-acetylpyridine. The series of thiosemicarbazides used to prepare the corresponding 2-acetylpyridine thiosemicarbazones (HApT; Figure 1) remained the same as that implemented to prepare the HDpT, HBpT, and HNBpT groups of Fe chelators.[5,7] This enabled variations in activity due to N4 substituents to be separated from those due to the substituent on the C-atom attached to the coordinated pyridine i.e., 2-pyridyl (HDpT), phenyl (HBpT), 3-nitrophenyl (HNBpT), and now methyl (HApT), by direct comparison of experiments done under the same conditions.[5,7] This approach has led to a very potent series of compounds with high Fe chelation efficacy and antiproliferative activity.

Results and Discussion

Syntheses and Spectroscopy. The HApT analogues were all prepared by high yielding, straightforward Schiff base condensation reactions leading to crystalline compounds that typically did not require further purification.

Structural Characterization. The crystal structures of HApT,[56] 2-acetylpyridine 4-methyl-3-thiosemicarbazone (HAp4mT),[57] 2-acetylpyridine 4-ethyl-3-thiosemicarbazone (HAp4eT),[58] 2-acetylpyridine 4-phenyl-3-thiosemicarbazone (HAp4pT)[59] and 2-acetylpyridine 4,4-dimethyl-3-thiosemicarbazone (HAp44mT)[60] are known. Herein, we have determined the structure of the remaining chelator from our series, namely 2-acetylpyridine 4-allyl-3-thiosemicarbazone (HAp4aT; Figure 2A), with the crystal data being presented in Table 1. The pairs of donor atoms (N1/N2 and N2/S1) are each in an anti orientation and the *E* isomeric form is observed. [The pyridyl ring and thiosemicarbazone NHCS moiety are on opposite sides of the C=N double bond.] All bond angles along the ligand backbone are close to 120°. A proton was identified on N3 from a difference electron density map during refinement. The C8−S1 bond (Table 2) is typical of a double bond, or in other words, the thioamide tautomer is present. An intramolecular H-bond

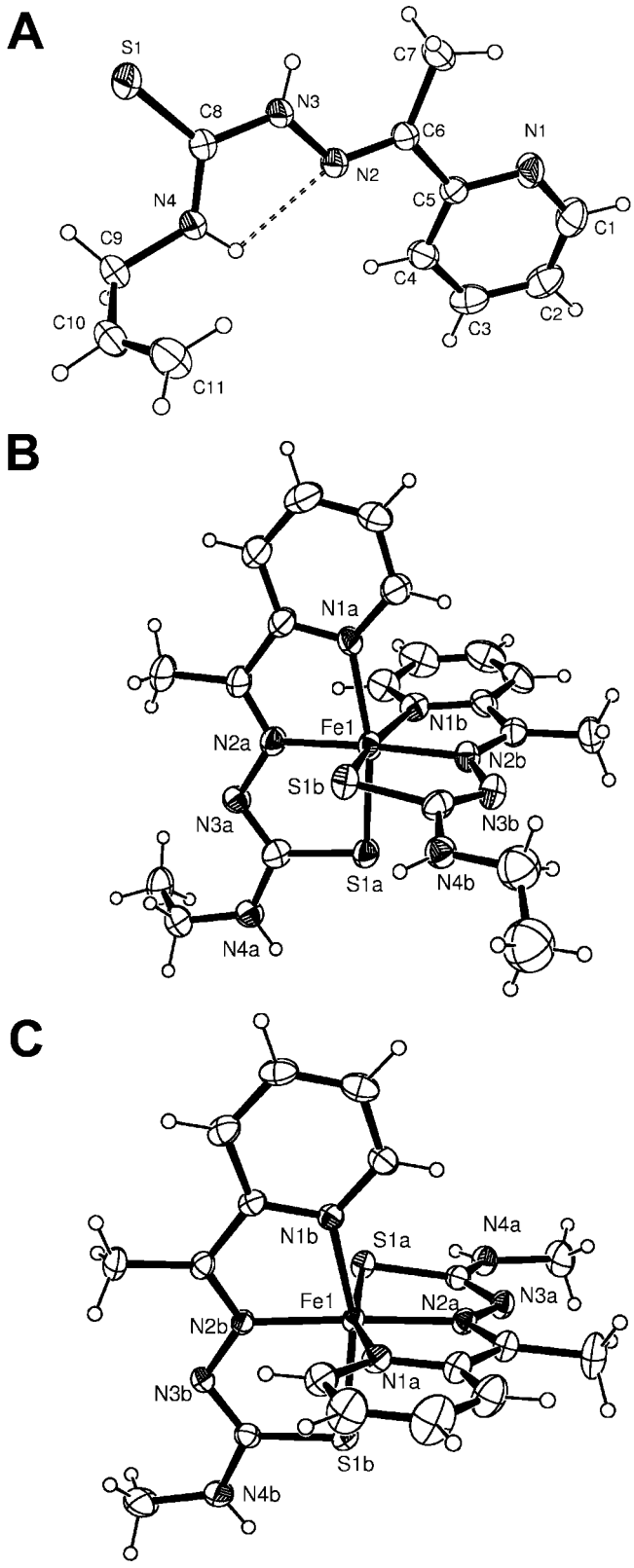

Figure 2. ORTEP views of (A) HAp4aT, (B) $[Fe(Ap4eT)_2]^+$ (ethyl group disorder not shown), and (C) $[Fe(Ap4mT)_2]^+$ (30% probability ellipsoids shown).

(N4−H···N2 2.18 Å, 108.5°) is also noted. In some cases, such as HAp44mT,[60] a different conformation of the thiosemicarbazone is preferred, where the donor atoms N1, N2, and S1, are all on the same side of the ligand backbone (the *E* (*syn*,*syn*) isomer). In this conformation, the three donor atoms are readily disposed to coordinate to a metal. Furthermore, in cases like this, a different tautomeric form is observed where the labile proton resides at N2 (formally the imine group) and not N3, as is normally found in thiosemicarbazone compounds and indeed for HAp4aT (Figure 2A).

Table 1. Crystal Data

	HAp4aT	$[Fe(Ap4eT)_2]ClO_4$	$[Fe(Ap4mT)_2]ClO_4$
formula	$C_{11}H_{14}N_4S$	$C_{20}H_{26}ClFeN_8O_4S_2$	$C_{18}H_{22}ClFeN_8O_4S_2$
formula weight	234.32	597.91	569.86
crystal system	triclinic	monoclinic	monoclinic
space group	*P*1 (no. 2)	$P2_1/c$ (no. 14)	$P2_1/c$ (no. 14)
color	colorless	black	black
a, Å	8.1372(7)	9.3038(5)	9.0780(6)
b, Å	8.6083(7)	13.8983(8)	13.4270(9)
c, Å	9.337(1)	20.5616(8)	19.860(1)
α, deg	76.842(8)		
β, deg	83.203(8)	99.330(4)	100.023(7)
γ, deg	71.007(8)		
V, Å^3	601.5(1)	2623.6(2)	2383.8(3)
T, K	293	293	293
Z	2	4	4
R_1 (obs data)	0.0382	0.0613	0.0443
wR_2 (all data)	0.0813	0.1413	0.1168
GOF	0.881	0.854	0.995

Table 2. Selected Bond Lengths (Å) and Angles (deg)

		$[Fe(Ap4eT)_2]ClO_4$[a]		$[Fe(Ap4mT)_2]ClO_4$[a]	
	HAp4aT	ligand *a*	ligand *b*	ligand *a*	ligand *b*
C8−S1	1.667(2)	1.755(6)	1.762(6)	1.753(3)	1.753(3)
C8−N3	1.365(2)	1.309(7)	1.304(7)	1.318(4)	1.318(4)
C8−N4	1.325(2)	1.334(7)	1.38(1)	1.337(4)	1.337(4)
N2−N3	1.362(2)	1.375(6)	1.378(6)	1.382(4)	1.382(4)
C6−N2	1.283(2)	1.297(7)	1.302(7)	1.311(4)	1.311(4)
Fe−N1		1.998(5)	1.982(5)	1.984(2)	1.984(2)
Fe−N2		1.914(4)	1.916(4)	1.924(2)	1.924(2)
Fe−S1		2.223(2)	2.215(2)	2.221(1)	2.221(1)
S1−Fe−N1		163.4(1)	163.6(1)	163.31(8)	163.31(8)
S1−Fe−N2		84.7(2)	84.87(8)	84.87(8)	84.87(8)
N1−Fe−N2		80.4(2)	80.2(2)	80.2(1)	80.2(1)
S1a−Fe−S1b		97.86(7)	98.29(4)		
N2a−Fe−N2b		176.0(2)	177.0(1)		

[a] The two columns of data refer to ligands *a* and *b*, respectively, i.e., C8*a*-S1*a* and C8*b*-S1*b*.

Considering bond length variations, the bonding within this tautomeric form may be rationalized by the three dipolar resonance forms shown in Figure 3B. By contrast, the more conventional thioamide form (Figure 3A) is simply represented by a single localized structure. The origin of these different tautomeric forms lies in the absence of a proton on N4 in the structure of HAp44mT, so no H-bonding of the kind illustrated in Figure 3A can take place. The imine N2 atom is evidently strongly nucleophilic and, in the absence of H-bonding with N4, captures a proton from N3, and the *cis*, *cis* conformation (Figure 3B) is observed. Indeed, all other structurally characterized HApT analogues in the literature, where N4 lacks a proton, exhibit this dipolar tautomeric form.[58,61−63]

However, the electronic influence of the methyl group attached to C6 is crucial in dictating the conformation and tautomeric form. Thiosemicarbazones derived from di-2-pyridyl ketone[64] and 2-benzoyl ketone,[65] where N4 is disubstituted, are found in the *Z* isomeric form shown in Figure 3C, where N3 is protonated and H-bonded to N1 in a completely different conformation. It then emerges that the electron-donating influence of the methyl group attached to C6 plays a role in raising the proton affinity of N2, while electron-withdrawing pyridyl and phenyl groups favor the *Z* isomer. Similarly, the corresponding 2-pyridineformamide thiosemicarbazones, where an electron donating primary amino group is bonded to C6 instead of a methyl group, always crystallize in the N2-protonated *E*(*syn*, *syn*) form if N4 bears no protons.[66,67]

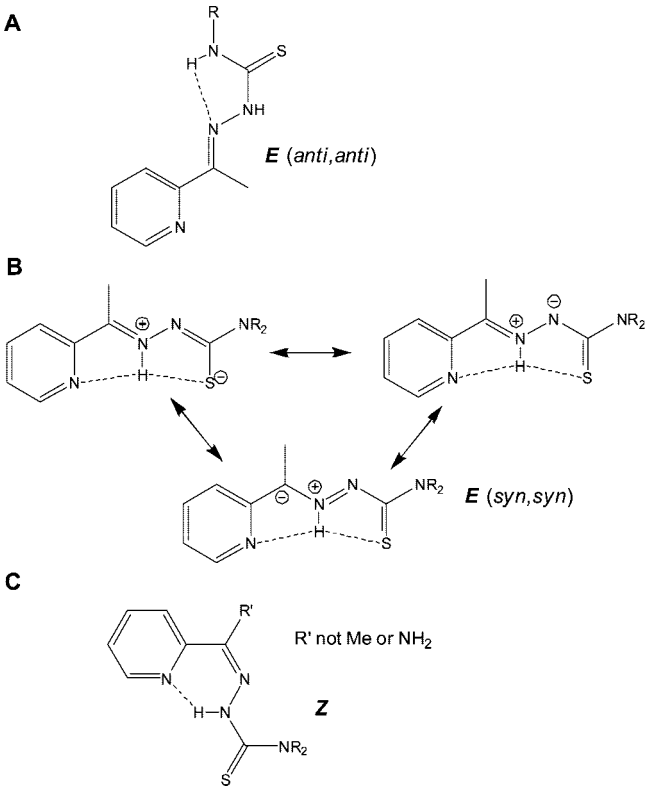

Figure 3. Different isomeric and tautomeric forms of pyridine thiosemicarbazones: (A) *E*(*anti*, *anti*), N3-protonated form, (B) *E*(*syn*, *syn*), N2-protonated form, and (C) the *Z* isomeric (N3-protonated) form.

The solution structures of thiosemicarbazones are solvent-dependent, and different isomeric (*E* or *Z*) forms may coexist in solution on the NMR time scale. It is known that strongly H-bonding solvents tend to favor a single isomeric form, as intramolecular H-bonding of the types shown in Figure 3 become less competitive than H-bonding with the solvent. In nonpolar solvents, multiple forms are often identified. In the present series of six thiosemicarbazones, HAp44mT is unique in exhibiting three sets of NMR resonances in DMSO-d_6, putatively from the *E*(*syn, syn*), *E*(*anti, anti*), and *Z* forms (Figure 3), while all other compounds reported here give a single set of resonances consistent with the *E*(*anti, anti*) isomer.

The crystal structures of the ferric complexes, [Fe(Ap4eT)$_2$]ClO$_4$ and [Fe(Ap4mT)$_2$]ClO$_4$, were also determined (Figure 2B,C). In both cases, the complex cation has approximate (but not crystallographic) 2-fold symmetry. Each ligand binds as a monoanionic *N*,*N*,*S* chelator in a meridional fashion, leading to an approximately orthogonal arrangement of the two ligands. As a consequence of deprotonation, the C8*n*−S1*n* bonds (formally double bonds in the free ligand) lengthen (Table 2), while the C8*n*−N3*n* bonds shorten; consistent with a dominantly ene-thiolate (−*N*═C−S$^-$) resonance form of the coordinated ligand (top left structure in Figure 3B). It is important that a lengthening of C8*n*−S1*n* and shortening of C8*n*−N3*n* in the complex is much greater than that seen in the zwitterionic free ligand, HAp44mT, where the C8−S1 and C8−N3 bonds were of intermediate bond order (between single and double bonds).[60]

The coordinate bonds are consistent with low spin Fe^{III} pyridyl thiosemicarbazone complexes[14,65] and is in contrast to the much longer coordinate bonds found in the high spin Fe^{III} complexes of aroylhydrazones such as 2-hydroxy-1-naphthaldehyde isonicotinoyl hydrazone (H$_2$NIH/311)[68] and pyridoxal isonicotinoyl hydrazone (H$_2$PIH).[69,70] This highlights the key influence of the S- and N-donor atoms of the thiosemicarbazones on their Fe coordination chemistry relative to the O,N,O donor set of H$_2$NIH and H$_2$PIH. The Fe−N and Fe−S bond lengths are also quite similar to those determined for the low spin Fe^{II} complex, Fe(NBp4eT)$_2$,[7] where the Fe^{II}−N1 and Fe^{II}−N2 bonds are ∼0.02−0.03 Å shorter than those found in ferric [Fe(Ap4mT)$_2$]ClO$_4$, while the Fe^{II}−S bonds are about ∼0.06 Å longer.

Table 3. Fe$^{III/II}$ Redox Potentials (mV *vs* NHE) of the [Fe(ApT)]$^+$ Analogues in MeCN:H$_2$O (7:3) in Comparison with Data Reported for the HDpT, HBpT, and HNBpT Fe Complexes[5,7]

Fe complex	E^o (mV *vs* NHE)
[Fe(ApT)$_2$]$^{+/0}$	+20
[Fe(Ap4mT)$_2$]$^{+/0}$	−3
[Fe(Ap44mT)$_2$]$^{+/0}$	+49
[Fe(Ap4eT)$_2$]$^{+/0}$	+23
[Fe(Ap4aT)$_2$]$^{+/0}$	+98
[Fe(Ap4pT)$_2$]$^{+/0}$	+63
[Fe(BpT)$_2$]$^{+/0}$	+120
[Fe(Bp4mT)$_2$]$^{+/0}$	+108
[Fe(Bp44mT)$_2$]$^{+/0}$	+119
[Fe(Bp4eT)$_2$]$^{+/0}$	+99
[Fe(Bp4aT)$_2$]$^{+/0}$	+117
[Fe(Bp4pT)$_2$]$^{+/0}$	+180
[Fe(DpT)$_2$]$^{+/0}$	+165
[Fe(Dp4mT)$_2$]$^{+/0}$	+153
[Fe(Dp44mT)$_2$]$^{+/0}$	+166
[Fe(Dp4eT)$_2$]$^{+/0}$	+173
[Fe(Dp4aT)$_2$]$^{+/0}$	+170
[Fe(Dp4pT)$_2$]$^{+/0}$	+225
[Fe(NBpT)$_2$]$^{+/0}$	+189
[Fe(NBp4mT)$_2$]$^{+/0}$	+185
[Fe(NBp44mT)$_2$]$^{+/0}$	unstable
[Fe(NBp4eT)$_2$]$^{+/0}$	+170
[Fe(NBp4aT)$_2$]$^{+/0}$	+187
[Fe(NBp4pT)$_2$]$^{+/0}$	+249

Electrochemistry. As our recent studies have shown that the redox activity of an Fe complex is associated with cytotoxicity of the chelator and thus its biological activity,[5,7] it was important to study the electrochemistry of the HApT Fe complexes. All compounds exhibited totally reversible Fe$^{III/II}$ couples in MeCN/H$_2$O (70:30). This solvent mixture was necessary due to the limited aqueous solubility of the complexes. The same voltammograms were obtained regardless of whether the Fe^{II} or Fe^{III} complex was employed, as expected for a facile, reversible, single electron redox process. The redox potentials are collated in Table 3.

The cathodic shift in the Fe$^{III/II}$ redox potentials of the HApT complexes in comparison to their corresponding HBpT, HDpT, and HNBpT Fe complexes is apparent from Figure 4 and Table 3. As an example, the voltammogram of [Fe(Ap4mT)$_2$]$^{+/0}$ is shown in Figure 4 in comparison with data from [Fe(Dp4mT)$_2$]$^{+/0}$, [Fe(Bp4mT)]$^{+/0}$, and [Fe(NBp4mT)]$^{+/0}$.

It is significant to note that the HApT series Fe complexes have the lowest Fe$^{III/II}$ redox potentials of any thiosemicarbazone series studied by our group to date and this may have significant implications on their biological activity. These Fe$^{III/II}$ redox potentials lie within a range accessible to both cellular oxidants and reductants (see below), and both the ferric and ferrous forms are chemically stable. Remembering that all four complexes in Figure 4 have identical substituents at N4 (a single methyl group), the differences in redox potential are only due to variations in the substituent on the C6 atom (using the numbering scheme from the crystal structures in Figure 2). The inductive effects of these groups span the range from electron-

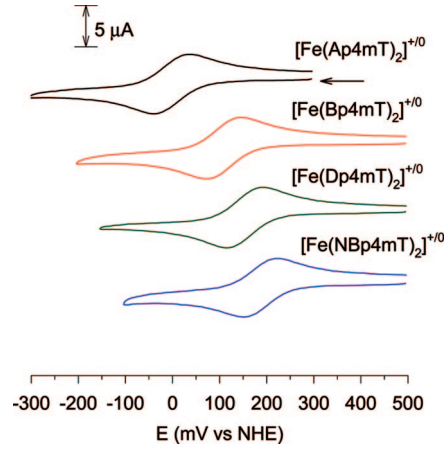

Figure 4. Cyclic voltammograms of $[Fe(Ap4mT)_2]^+$ (black), $[Fe(Bp4mT)_2]^+$ (red), $[Fe(Dp4mT)_2]^+$ (green), and $[Fe(Bp4mT)_2]^+$ (blue). Experimental conditions were 1 mM concentrations of complex in MeCN:H_2O (70:30) and 0.1 M Bu_4NClO_4 using a sweep rate 100 mV s^{-1}. All sweeps were initiated in direction of the arrow.

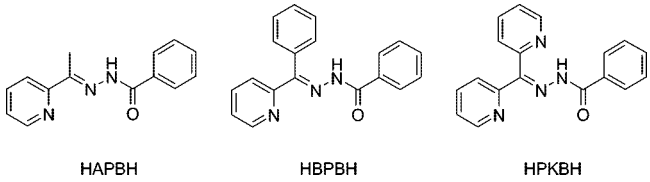

Figure 5. Line drawings of the hydrazones HAPBH, HBPBH, and HPKBH.

donating (methyl) through to strongly electron-withdrawing (3-nitrophenyl), and their influence on the $Fe^{III/II}$ redox potentials are consistent with this. The shift in $Fe^{III/II}$ redox potential observed by varying the C6 substituent from methyl to 3-nitrophenyl (*ca.* 170 mV) outweigh those of variations in the N4 substituent (from methyl to phenyl spanning a range of *ca.* 60 mV). The greater sensitivity of the redox potential to the effect of the C6 substituent no doubt relates to its closer proximity to the metal than the N4 group.

Similar inductive effects on $Fe^{III/II}$ redox potentials were previously observed in the complexes of the related hydrazone analogues, 2-acetylpyridine benzoyl hydrazone (HAPBH; Figure 5), 2-benzoylpyridine benzoyl hydrazone (HBPBH; Figure 5), and dipyridylketone benzoyl hydrazone (HPKBH; Figure 5).[71] The main differences in comparison with the present thiosemicarbazone Fe complexes were due to the (N,N,O) donor set of the hydrazones, which shifted the $Fe^{III/II}$ redox potentials to the range +300 to +500 mV *vs* NHE.[71] This highlights the importance of the terminal substituents adjacent to the coordinating S- or O-donor with regards to the resulting Fe complex redox potential.

Ascorbate Oxidation Assay. If a complex undergoes redox cycling between its Fe^{II} and Fe^{III} forms in oxygenated solution, the formation of the superoxide radical as the single electron reduction product of O_2 is likely. Similarly, reaction between Fe^{II} and H_2O_2 may lead to the production of hydroxyl radicals ($^{\bullet}OH$) through so-called Fenton chemistry.[72] In both cases, these reactive oxygen species are potentially damaging to biomolecules within the cell. In the present case, these processes may play a role in the antitumor effects of the chelators through formation of intracellular Fe complexes.[5,7] It could be suggested that the low potential ferrous HApT complexes will be more rapidly oxidized than the corresponding HBpT, HDpT, and HNBpT analogues. Conversely, it may be expected that the ferric complexes of the HApT ligands will react more slowly with intracellular reductants than the other higher potential analogues. In other words, either half-reaction may be rate-limiting and an optimal potential window will be expected where both the oxidative and reductive half-reactions are rapid.

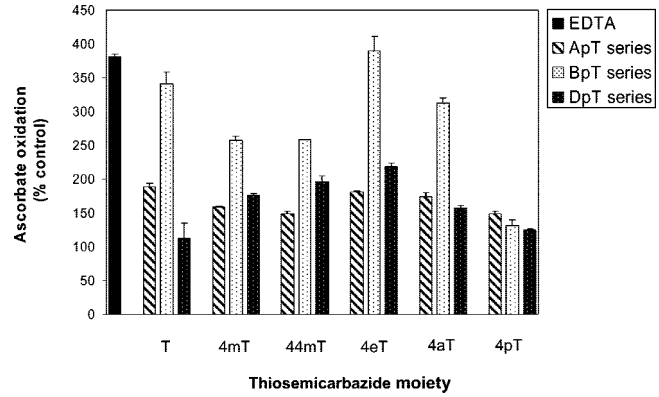

Figure 6. Oxidation of ascorbate by the Fe complexes of the HApT, HBpT, and HDpT analogues compared to EDTA at an IBE of 3. In all cases, the ferric $[FeL_2]^+$ complex is the active oxidant. Activity is shown as a percentage relative to ferric citrate (no additional chelator present). See Experimental Procedures for further details. Results are mean ± SD of three experiments.

The ability of the complexes to be reduced by biologically relevant molecules may be assessed in a chemical assay whereby the Fe complexes are incubated with ascorbate in aerated aqueous solution.[5,73] Upon reduction of the ferric complexes by ascorbate, aerial reoxidation sustains a catalytic ascorbate oxidation cycle.

The ascorbate oxidation assay was performed at Fe-binding equivalents (IBE) of 0.1, 1, and 3. At an IBE of 0.1, little effect on ascorbate oxidation was noted, while similar results were observed at IBEs of 1 and 3. For clarity, we have only presented the results at an IBE of 3 (Figure 6), which represents an excess of chelator to Fe (see Experimental Procedures) and was chosen to better reflect the pharmacological excess of chelator to Fe that would occur in vivo. Additionally, the well described chelator, EDTA, was used as a positive control, which was observed to increase ascorbate oxidation markedly (Figure 6), in agreement with previous studies.[73,74]

The oxidative half-reaction (oxidation of ascorbate) should be more rapid for complexes with higher $Fe^{III/II}$ redox potentials (all other parameters being equal). The redox potential of the two-electron ascorbate/dehydroascorbate couple at pH 7.2 is +60 mV *vs* NHE.[75] This value is in the same range as the redox potentials of the Fe complexes of the HApT analogues (Table 3), thus there is very little driving force for the reaction compared with the higher potential Fe complexes of the HDpT and HBpT analogues.

The ascorbate oxidation assay results of the Fe complexes of the HApT, HDpT, and HBpT analogues (Figure 6) show an interesting trend. The $[Fe(BpT)_2]^+$ analogues are the fastest ascorbate oxidation catalysts, although their $Fe^{III/II}$ redox potentials are intermediate of the $[Fe(ApT)_2]^+$ (lowest) and $[Fe(DpT)_2]^+$ (highest) complexes.[5,7] As discussed above, the fact that $[Fe(ApT)_2]^+$ analogues are poorer ascorbate reduction catalysts than the corresponding $[Fe(BpT)_2]^+$ complexes may be ascribed to their slow reduction by ascorbate that is inhibited by their low $Fe^{III/II}$ redox potentials. Because the $[Fe(BpT)_2]^+$ complexes are better ascorbate oxidation catalysts than their higher potential $[Fe(DpT)_2]^+$ analogues, this indicates that the reductive half-reaction (i.e., $Fe^{II}(DpT)_2 + O_2$) is slow and rate-limiting due to the higher potential $Fe(DpT)_2$ complexes.

Table 4. Inhibition of Proliferation of SK-N-MC Cells by the HApT Series of Chelators Compared to Relevant Positive Control Chelators after a 72 h Incubation[a]

ligand (HL)	partition coefficient of free ligand (log*P*)	IC_{50} (μM) of free ligand	IC_{50} (μM) of $Fe^{II}L_2$ complex	IC_{50} (μM) of $[Fe^{III}L_2]ClO_4$ complex
DFO		7.35 ± 1.53		
H_2NIH (311)		0.50 ± 0.04		
HDp44mT	2.19	0.002 ± 0.001		
HBp4eT	4.01	0.003 ± 0.001		
HApT	1.52	3.53 ± 0.60	>6.25	>6.25
HAp4mT	2.70	0.011 ± 0.001	0.15 ± 0.01	0.15 ± 0.03
HAp44mT	1.80	0.001 ± 0.001	0.04 ± 0.01	0.02 ± 0.01
HAp4eT	1.52	0.002 ± 0.001	0.05 ± 0.01	0.06 ± 0.04
HAp4aT	1.76	0.001 ± 0.001	0.05 ± 0.02	0.29 ± 0.04
HAp4pT	2.99	0.001 ± 0.001	0.08 ± 0.01	0.09 ± 0.01

[a] The results are mean ± SD (three experiments).

These results indicate that $Fe^{III/II}$ redox potentials of the $Fe(BpT)_2$ complexes lie within the optimal potential window to catalyze the oxidation of ascorbate, where either half-reaction is rapid. On the other hand, these data suggest that the $Fe^{III/II}$ redox potentials of the $Fe(ApT)_2$ and $Fe(DpT)_2$ complexes approach either end of this window and are not as efficient as the $Fe(BpT)_2$ complexes in the oxidation of ascorbate. Nevertheless, the moderate ability of most $Fe(ApT)_2$ complexes to oxidize ascorbate suggests that the generation of reactive oxygen species may still play a role in their biological activity.

Anti-Proliferative Activity Against Tumor Cells: The HApT Chelators. The ability of the HApT series to inhibit cellular proliferation was assessed using SK-N-MC neuroepithelioma cells (Table 4), as the effect of many series of Fe chelators on their growth has been well characterized.[15,19,20] These novel ligands were compared to a number of relevant positive controls. These included DFO, which is used for the treatment of Fe overload,[2,3] and the well-described hydrazone, H_2NIH (311), which has moderate antiproliferative efficacy.[15,68] In addition, results were compared to two of the most active antiproliferative agents from the HBpT and HDpT series, namely HBp4eT and HDp44mT.[5,7]

This study identified four of the six HApT series of chelators (i.e., HAp44mT, HAp4eT, HAp4aT, and HAp4pT) as having potent antiproliferative activity (IC_{50}: 0.001−0.002 μM) that was similar to that observed with HBp4eT and HDp44mT and significantly ($p < 0.001$) greater than DFO or H_2NIH (Table 4). The parent analogue, HApT, was the least effective of the series, having an IC_{50} of 3.53 μM, which was still significantly ($p < 0.01$) more effective than DFO but less active than H_2NIH (Table 4). Of interest, the corresponding parent analogues of the HBpT, HDpT, and HNBpT series were also the least effective of their group, having similar IC_{50} values as HApT, namely 3.52−4.66 μM.[7] This could be related to the fact that these analogues, in each case, represent the most hydrophilic compounds of the relevant series. The ligand, HAp4mT, showed activity intermediate between HApT and the other four compounds in its series, having an IC_{50} of 0.011 μM (Table 4). Again, analogous compounds of the HDpT and HNBpT series (namely HDp4mT and HNBp4mT),[6,19] were also not highly effective, suggesting this substitution leads to nonoptimal efficacy.

The octanol:water partition coefficients of the six HApT free ligands are also listed in Table 4. There is an apparent optimal log*P* value between 1.5 and 2 for antiproliferative activity, while more hydrophilic or more hydrophobic compounds are not as potent. We have noted a similar correlation before.[5,7] The likely reason is that the most hydrophilic compounds will have difficulty crossing the cell membrane, while very hydrophobic analogues may become entrapped within membranes through a high affinity for the lipid environment.

Anti-Proliferative Activity Against Tumor Cells: The Fe Complexes of the HApT Series. Previous studies have illustrated that complexation of related aroylhydrazone[76−78] and thiosemicarbazone[79] chelators with metal ions can result in marked changes in their biological activity. Such experiments address the question of whether the sole mode of action is due to the ability of a chelator to bind Fe intracellularly or whether other mechanisms are also relevant. To determine the effect of complexation on the antiproliferative behavior of the HApT series, their Fe^{II} and Fe^{III} complexes were synthesized and the antiproliferative activity was examined using SK-N-MC neuroepithelioma cells. In comparison with their free ligands, the Fe^{II} and Fe^{III} complexes of all HApT analogues demonstrated significantly ($p < 0.001$) decreased antiproliferative activity (Table 4). In fact, complexation resulted in a 14−290-fold increase of the IC_{50} value.

Assessing the difference in IC_{50} values between the Fe^{II} and Fe^{III} complexes, the antiproliferative activity of each component of the redox pair was the same within experimental uncertainty except HAp4aT, where the IC_{50} of the Fe^{III} complex was 6-fold higher than that of the Fe^{II} complex (Table 4). It is notable that all Fe^{II} complexes of the HApT analogues were prepared under an inert atmosphere and they slowly oxidize to their ferric complex in aerated aqueous solutions (conditions under which our assays were performed). Electrochemistry has identified significantly lower $Fe^{III/II}$ redox potentials of the HApT complexes, relative to the corresponding Fe complexes from the HDpT and HBpT series, which is consistent with the greater air sensitivity of their Fe^{II} complexes that we observe. The similarities between the biological activities of the Fe^{II} and Fe^{III} complexes of the HApT analogues suggests they each equilibrate to the same ratio of Fe^{III} and Fe^{II} species depending on the intracellular potential.

It is notable that precomplexation with Fe did not totally prevent antiproliferative activity of the five most potent HApT series ligands (Table 4). This result was similar to data obtained with the most potent chelators of the HBpT, HDpT, and HNBpT series[5,6] and probably can be explained by the fact that the Fe complexes are cytotoxic, probably due to their redox activity.[5,19] However, the fact that the Fe complexes are significantly less cytotoxic than their corresponding chelators is interesting and may be due to several possible factors. Precomplexation with Fe inhibits the ability of the chelator to sequester intracellular Fe that is crucial for cellular proliferation. Also, the Fe complex (in its ferric form) may be less able to gain entry to the cell than the smaller and charge neutral ligand on the basis of acid dissociation constants determined earlier.[5] For example, the HDpT analogues are all charge neutral across a wide pH range (*ca.* 4 < pH < 9) regardless of the N4 substituent.[5] The ferric complexes of these chelators will always bear a positive charge, and this may impair their ability to cross the cell membrane.

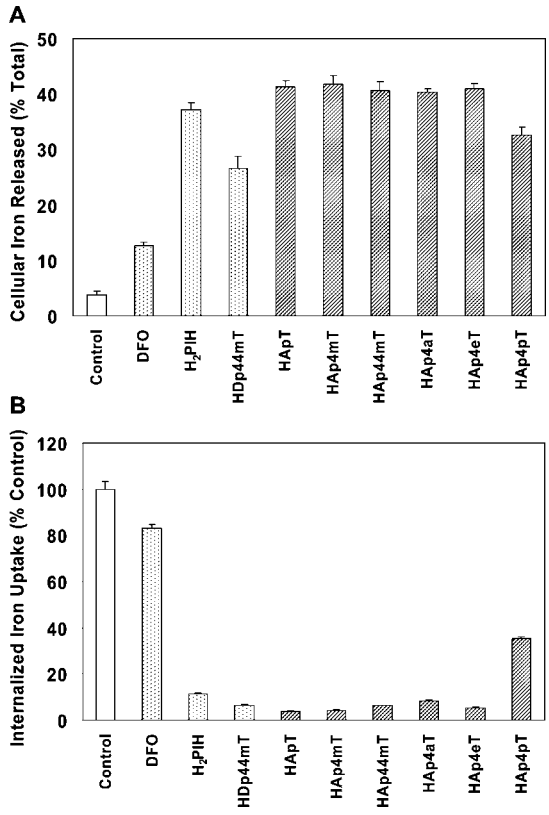

Figure 7. The effect of the HApT series chelators on: (A) ^{59}Fe mobilization from prelabeled SK-N-MC neuroepithelioma cells and (B) ^{59}Fe uptake from ^{59}Fe-transferrin (^{59}Fe$_2$-Tf) by SK-N-MC neuroepithelioma cells. Data for DFO, H_2PIH, and HDp44mT are shown for comparison. Control experiments were carried out in the absence of any chelator. See Experimental Procedures for further details. Results are mean ± SD of three experiments with three determinations in each experiment.

The Fe^{II} complexes are, like the free ligand, charge neutral but also susceptible to oxidation to their ferric analogue.

Cellular Fe Efflux. In an effort to understand the mechanisms of action of the HApT series, initial experiments characterized the ability of these chelators to mobilize intracellular ^{59}Fe from prelabeled SK-N-MC neuroepithelioma cells (Figure 7A). The release of ^{59}Fe mediated by these ligands was compared to that of a number of positive controls, including DFO, H_2PIH, and HDp44mT (Figure 1), which have been characterized in detail.[15,19,80]

Both H_2PIH and HDp44mT showed high ^{59}Fe mobilization activity, releasing 37 ± 1% and 27 ± 2% of intracellular ^{59}Fe (Figure 7A), respectively, as shown previously.[80−82] In comparison, the control (culture medium alone) mediated 4 ± 1% of intracellular ^{59}Fe release. In accordance with previous studies,[6,7] the clinically used chelator, DFO, demonstrated poor ^{59}Fe mobilization efficacy, resulting in the release of only 13 ± 1% of intracellular ^{59}Fe (Figure 7A). All members of the HApT series led to significant ^{59}Fe mobilization activity, resulting in the release of 33−42% of cellular ^{59}Fe. The least effective analogue was HAp4pT that released 33% of cellular ^{59}Fe, with the remaining five HApT analogues showing very similar activity, resulting in mobilization of 40−42% of cellular ^{59}Fe (Figure 7A). These latter compounds were significantly ($p < 0.001$) more effective than DFO or HDp44mT, while HAp4pT ($p < 0.001$) was significantly more effective than DFO. Interestingly, assessing previous series of chelators, the analogous ligands to HAp4pT, namely HBp4pT, HNBp4pT, and HDp4pT, all generally showed lower Fe mobilization activity than most other analogues in their respective series. This indicates some unfavorable factor with these analogues (e.g., lipophilicity etc.), suggesting this substituent should be avoided in future ligand design. The chelator-mediated increase in cellular ^{59}Fe mobilization was not mediated by their cytotoxic effects, as the cells remained viable within the short 3 h incubation used.

Inhibition of Cellular ^{59}Fe Uptake from ^{59}Fe-Transferrin. The ability of the HApT series chelators to inhibit ^{59}Fe uptake from the serum Fe-binding protein, diferric transferrin (Fe_2-Tf), in SK-N-MC neuroepithelioma cells was also assessed (Figure 7B). This is important, as inducing Fe-deprivation and antiproliferative activity in culture involves both increasing cellular Fe mobilization and preventing Fe uptake from Fe_2-Tf into the cell.[15] As demonstrated in our previous studies,[19,80] the positive controls, H_2PIH and HDp44mT, were found to effectively reduce ^{59}Fe uptake to 11 ± 1% and 7 ± 1% of the control, respectively (Figure 7B). In contrast, the hydrophilic chelator, DFO, exhibited poor ability to decrease ^{59}Fe uptake, reducing it to only 83 ± 2% of the control (Figure 7B), as shown previously.[6,7,19]

As found in the complementary ^{59}Fe efflux experiments (Figure 7A), the least effective HApT analogue was HAp4pT that reduced ^{59}Fe uptake to only 35 ± 1% of the control (Figure 7B). This ligand was significantly ($p < 0.001$) more effective than DFO but significantly less active than H_2PIH, HDp44mT, and the remainder of the HApT series of chelators. In fact, the remaining HApT ligands reduced ^{59}Fe uptake to 4−8% of the control, having activity similar to HDp44mT and being significantly more effective than H_2PIH and DFO (Figure 7B). It is notable that H_2PIH and HDp44mT have been among the most potent Fe chelators we have studied[15,82,83] and thus the present compounds demonstrate high Fe chelation efficacy.

Efficacy of the HApT Chelators to Directly Remove ^{59}Fe from ^{59}Fe-Transferrin. The ability of the chelators to inhibit ^{59}Fe uptake from the plasma protein ^{59}Fe$_2$-Tf (Figure 7B) could, in principle, be due to their ability to remove ^{59}Fe directly from ^{59}Fe$_2$-Tf before internalization via the process of receptor-mediated endocytosis.[1] To examine this, ^{59}Fe$_2$-Tf (0.75 μM) was incubated with the chelators (25 μM) under the same conditions used in Fe uptake experiments, that is, for 3 h at 37 °C. The solutions were then dialyzed and the release of ^{59}Fe into the dialysate determined.

In the absence of chelators, very little ^{59}Fe was released, namely 1.3 ± 0.3% (Table 5). The chelators, DFO and deferiprone (L1), were used as positive controls because they are known[83,84] to remove ^{59}Fe from ^{59}Fe$_2$-Tf and led to the release of 14% and 20% of ^{59}Fe, respectively. Considering previous studies of the structurally related HBpT and HDpT analogues and their ability to reduce cellular ^{59}Fe uptake from ^{59}Fe$_2$-Tf,[7,19] their activity was compared to the HApT series. All HDpT, HBpT, and HApT series chelators had little effect on the direct release of ^{59}Fe from ^{59}Fe$_2$-Tf, resulting in mobilization of 0.9−4.4% of ^{59}Fe (Table 5). Hence, the marked ability of the HApT (Figure 7B), HBpT, and HDpT ligands at preventing ^{59}Fe uptake from ^{59}Fe$_2$-Tf by cells is not due to their ability to directly remove ^{59}Fe from this protein.

Conclusions

Thiosemicarbazones are an important group of Fe chelators that show potent and selective antitumor activity.[5,7,8,14,60,79] Their ability to bind Fe and other metals is vital for their antiproliferative efficacy and elucidation of the structure−activity

Table 5. Release of Transferrin-Bound ^{59}Fe by Iron Chelators as Measured Using Dialysis Experiments (see *Experimental Procedures* for Details)[a]

ligand	^{59}Fe removed from $^{59}Fe_2$-Tf (% total)
control	1.3 ± 0.3
L1	20.0 ± 2.0
DFO	14.2 ± 3.0
HDpT	1.6 ± 0.2
HDp4mT	1.9 ± 0.1
HDp44mT	2.9 ± 0.2
HDp4eT	2.0 ± 0.1
HDp4aT	2.0 ± 0.1
HDp4pT	2.0 ± 0.2
HBpT	2.0 ± 0.1
HBp4mT	2.2 ± 0.1
HBp44mT	2.7 ± 0.1
HBp4eT	3.1 ± 0.2
HBp4aT	3.5 ± 0.2
HBp4pT	4.4 ± 0.3
HApT	1.0 ± 0.1
HAp4mT	1.8 ± 0.6
HAp44mT	2.7 ± 0.6
HAp4eT	2.1 ± 0.4
HAp4aT	1.7 ± 0.4
HAp4pT	0.9 ± 0.2

[a] The results are mean ± SD (three experiments).

relationships of this group of compounds is important to develop increasingly active and selective anticancer agents.

The current study highlights structure−activity relationships critical for the antitumor activity of thiosemicarbazones. In fact, we demonstrate the significance of substituents positioned at the imine carbon (C6) and the consequential effect on antiproliferative activity. The inductive effects of groups at this position were observed to influence the $Fe^{III/II}$ redox potentials due to their proximity to the metal center. Those series of chelators containing an electron-withdrawing substituent e.g., HNBpT series, exhibited higher $Fe^{III/II}$ redox potentials.[7] The Fe complexes of the HApT series, which have an electron-donating methyl substituent at C6, demonstrated the lowest $Fe^{III/II}$ redox potentials of any thiosemicarbazone series investigated by our laboratories. Nevertheless, the HApT analogues maintained the ability to oxidize ascorbate, having activity comparable to the HDpT series but less than the HBpT analogues. However, in general, the HApT series showed marked antiproliferative activity. This suggests that other factors, such as Fe chelation activity and lipophilicity, are significant in terms of their efficacy.

Considering the above conclusion, an important observation from this study was the general potent Fe chelation efficacy of the HApT analogues. This property is somewhat in contrast to the HBpT and HDpT series of compounds, where some of these ligands (e.g., HDpT or HBp4pT) showed less Fe chelation activity.[7,19] Significantly, four of the six HApT chelators demonstrated potent antitumor activity (IC_{50}: 0.001−0.002 μM) that was comparable to the most effective HBpT and HDpT ligands. This makes the HApT series among the most active anticancer agents developed by our laboratories to date.

Experimental Procedures

Reagents. All commercial reagents were used without further purification. Desferrioxamine (DFO) was obtained from Novartis (Basel, Switzerland). The chelators, HBp4eT, HDp44mT, H_2NIH, and H_2PIH were prepared and characterized according to previously described methods.[5,7,68]

Syntheses. See Supporting Information for full characterization data.

Chelators of the HApT Series: General Synthesis. 2-Acetylpyridine (1.15 g, 0.01 mol) was dissolved in 15 mL ethanol, and then 1.00 g (0.01 mol) of the appropriate thiosemicarbazide dissolved in warm water (15 mL) was added. Glacial acetic acid (5−6 drops) was added, and the mixture was gently refluxed for 2 h. The mixture was cooled to room temperature and then allowed to stand in a refrigerator overnight to ensure complete precipitation. The product was filtered off and washed with ethanol (10 mL) followed by diethyl ether (10 mL).

2-Acetylpyridine thiosemicarbazone (HApT). Colorless crystals (yield: 81%).

2-Acetylpyridine 4-methyl-3-thiosemicarbazone (HAp4mT). Colorless crystals (yield: 73%).

2-Acetylpyridine 4-allyl-3-thiosemicarbazone (HAp4aT). Colorless crystals (yield: 80%).

2-Acetylpyridine 4-phenyl-3-thiosemicarbazone (HAp4pT). Colorless crystals (yield: 81%).

2-Acetylpyridine 4,4-dimethyl-3-thiosemicarbazone (HAp44mT). Yellow needles (yield: 67%).

2-Acetylpyridine 4-ethyl-3-thiosemicarbazone (HAp4eT). Colorless crystals (yield: 83%).

Fe^{III} Complexes: $[FeL_2]ClO_4$ (Where $L^- =$ ApT Analogue Monoanion). The complexes were prepared by the following general method. The appropriate thiosemicarbazone (3.6 mmol) was dissolved in ethanol (15 mL), and 0.37 g (3.6 mmol) of triethylamine was added to the solution. Solid $Fe(ClO_4)_3 \cdot 6H_2O$ (1.8 mmol, 0.849 g) was added directly to the basic ligand solution, and the mixture was gently refluxed for 30 min. Upon cooling, the product was filtered off and washed with ethanol (10 mL) followed by diethyl ether (10 mL).

$[Fe(ApT)_2]ClO_4$. Dark-brown powder (yield: 91%). Electronic spectrum (MeOH): λ_{max} (nm) (ε, L mol^{-1} cm^{-1}) 465 (6990), 367 (16600).

$[Fe(Ap4mT)_2]ClO_4$. Black powder (yield: 49%). Electronic spectrum (MeOH): λ_{max} (nm) (ε, L mol^{-1} cm^{-1}) 466 (3300), 364 (11600).

$[Fe(Ap4aT)_2]ClO_4$. Brown powder (yield: 66%). Electronic spectrum (MeOH): λ_{max} (nm) (ε, L mol^{-1} cm^{-1}) 510 (2750), 358 (12500).

$[Fe(Ap4pT)_2]ClO_4 \cdot 1^1/_2H_2O$. Brown powder (yield: 79%). Electronic spectrum (MeOH): λ_{max} (nm) (ε, L mol^{-1} cm^{-1}) 508 (3410), 390 (36200).

$[Fe(Ap44mT)_2]ClO_4$. Brown powder (yield: 56%). Electronic spectrum (MeOH): λ_{max} (nm) (ε, L mol^{-1} cm^{-1}) 509 (3100), 380 (14000).

$[Fe(Ap4eT)_2]ClO_4$. Brown powder (yield: 72%). Electronic spectrum (MeOH): λ_{max} (nm) (ε, L mol^{-1} cm^{-1}) 509 (2300), 371 (13000).

Fe^{II} Complexes: $Fe^{II}L_2$ (Where $L^- =$ ApT Analogue Monoanion). The Fe complexes were prepared by the following general method. The thiosemicarbazone (3.5 mmol) was dissolved in ethanol (15 mL). Triethylamine (0.36 g, 3.6 mmol) was added to the solution, and the mixture was purged with nitrogen. Solid $Fe(ClO_4)_2 \cdot 6H_2O$ (0.652 g, 1.8 mmol) was added directly to the ligand solution, and the mixture was gently refluxed for 30 min under nitrogen. Upon cooling, the product was filtered off and washed with ethanol (10 mL) followed by diethyl ether (10 mL).

$[Fe(ApT)_2] \cdot H_2O$. Black powder (yield: 78%). Electronic spectrum (MeOH): λ_{max} (nm) (ε, L mol^{-1} cm^{-1}) 634 (1790), 366 (12500).

$[Fe(Ap4mT)_2] \cdot H_2O$. Green powder (yield: 85%). Electronic spectrum (MeOH): λ_{max} (nm) (ε, L mol^{-1} cm^{-1}) 626 (735), 366 (15400).

$Fe(Ap4aT)_2$. Green powder (yield: 76%). Electronic spectrum (MeOH): λ_{max} (nm) (ε, L mol^{-1} cm^{-1}) 634 (1130), 360 (14900).

$[Fe(Ap4pT)_2] \cdot H_2O$. Green powder (yield: 87%). Electronic spectrum (MeOH): λ_{max} (nm) (ε, L mol^{-1} cm^{-1}) 630 (925), 389 (20900).

$[Fe(Ap44mT)_2] \cdot 1^1/_4H_2O$. Green powder (yield: 83%). Electronic spectrum (MeOH): λ_{max} (nm) (ε, L mol^{-1} cm^{-1}) 632 (515), 381 (20200).

$Fe(Ap4eT)_2$. Green powder (yield: 85%). Electronic spectrum (MeOH): λ_{max} (nm) (ε, L mol^{-1} cm^{-1}) 632 (1080), 364 (24700).

Physical Methods. ^{1}H NMR (400 MHz) spectra were acquired using a Bruker Avance 400 NMR spectrometer with DMSO-d_6 as the solvent and internal reference (Me_2SO: ^{1}H NMR δ 2.49 ppm and ^{13}C NMR δ 39.5 ppm *vs* TMS). Infrared spectra were measured on undiluted solid samples with a Perkin-Elmer FT-IR spectrophotometer equipped with an attenuated total reflectance assembly. Cyclic voltammetry was performed using a BAS100B/W potentiostat. A glassy carbon working electrode, an aqueous Ag/AgCl reference, and Pt wire auxiliary electrode were used. All complexes were at *ca*. 1 mM concentration in MeCN:H_2O 70:30 v/v. This solvent combination was used to ensure solubility of all compounds. The supporting electrolyte was Et_4NClO_4 (0.1 M), and the solutions were purged with nitrogen prior to measurement. All potentials are cited versus the normal hydrogen electrode (NHE) by addition of 196 mV to the potentials measured relative to the Ag/AgCl reference. Partition coefficients of the free ligands were determined as previously described.[85]

Crystallography. Crystallographic data were acquired at 293 K on an Oxford Diffraction Gemini CCD diffractometer employing graphite-monochromated Mo Kα radiation (0.71073 Å) and operating within the range $2 < 2\theta < 50$ Å. Data reduction and empirical absorption corrections (multiscan) were performed with Oxford Diffraction CrysAlisPro software. Structures were solved by direct methods with SHELXS and refined by full-matrix least-squares analysis with SHELXL-97.[86] All non-H atoms were refined with anisotropic thermal parameters. Molecular structure diagrams were produced with ORTEP3.[87] These data in CIF format have been deposited at the Cambridge Crystallographic Data Centre with deposition numbers CCDC 713027−713029.

Biological Studies. Cell Culture. Chelators were dissolved in DMSO as 10 mM stock solutions and diluted in medium containing 10% fetal calf serum (Commonwealth Serum Laboratories, Melbourne, Australia) so that the final [DMSO] < 0.5% (v/v). The human SK-N-MC neuroepithelioma cell line (American Type Culture Collection, Manassas, VA) was grown as previously described[15] at 37 °C in a humidified atmosphere of 5% CO_2/95% air in an incubator (Forma Scientific, Marietta, OH).

Effect of the Chelators and Complexes on Cellular Proliferation. The effect of the chelators and complexes on cellular proliferation were determined by the MTT [1-(4,5-dimethylthiazol-2-yl)-2,5-diphenyl tetrazolium] assay using standard techniques.[7,15] The SK-N-MC cell line was seeded in 96-well microtiter plates at 1.5×10^4 cells/well in medium containing human Fe_2-Tf (1.25 μM) and chelators or complexes at a range of concentrations (0−6.25 μM). Control samples contained medium with Fe_2-Tf (1.25 μM) without the ligands. The cells were incubated at 37 °C in a humidified atmosphere containing 5% CO_2 and 95% air for 72 h. After incubation, 10 μL of MTT (5 mg/mL) was added to each well and further incubated at 37 °C for 2 h. After solubilization of the cells with 100 μL of 10% SDS-50% isobutanol in 10 mM HCl, the plates were read at 570 nm using a scanning multiwell spectrophotometer. The results, which are the means of three experiments, are expressed as a percentage of the control. The inhibitory concentration (IC_{50}) was defined as the chelator or complex concentration necessary to reduce the absorbance to 50% of the untreated control. Using this method, absorbance was shown to be directly proportional to cell counts, as shown previously.[15]

Preparation of ^{59}Fe-Transferrin. Human Tf (Sigma) was labeled with ^{59}Fe (Dupont NEN, MA) to produce $^{59}Fe_2$-Tf, as previously described.[88,89] Unbound ^{59}Fe was removed by exhaustive vacuum dialysis against a large excess of 0.15 mM NaCl buffered with 1.4% $NaHCO_3$ by standard methods.[88,89]

Effect of Chelators on ^{59}Fe Efflux from Cells. Iron efflux experiments examining the ability of various chelators to mobilize ^{59}Fe from SK-N-MC cells were performed using established techniques.[6,7,15] Briefly, following prelabeling of cells with $^{59}Fe_2$-Tf (0.75 μM) for 3 h at 37 °C, the cell cultures were washed four times with ice-cold PBS and then subsequently incubated with each chelator (25 μM) for 3 h at 37 °C. The overlying media containing released ^{59}Fe was then separated from the cells using a Pasteur pipet. Radioactivity was measured in both the cell pellet and supernatant using a γ-scintillation counter (Wallac Wizard 3, Turku, Finland). In these studies, the novel ligands were compared to the previously characterized chelators, DFO, H_2PIH, and HDp44mT.

Effect of Chelators at Preventing ^{59}Fe Uptake from $^{59}Fe_2$-Tf by Cells. The ability of the chelator to prevent cellular ^{59}Fe uptake from the serum Fe transport protein, $^{59}Fe_2$-Tf, was examined using established techniques.[6,7,15] Briefly, cells were incubated with $^{59}Fe_2$-Tf (0.75 μM) for 3 h at 37 °C in the presence of each of the chelators (25 μM). The cells were then washed four times with ice-cold PBS, and internalized ^{59}Fe was determined by standard techniques by incubating the cell monolayer for 30 min at 4 °C with the general protease, Pronase (1 mg/mL; Sigma). The cells were removed from the monolayer using a plastic spatula and centrifuged for 1 min at 14000 rpm. The supernatant represents membrane-bound, Pronase-sensitive ^{59}Fe that was released by the protease, while the Pronase-insensitive fraction represents internalized ^{59}Fe. The novel ligands were compared to the previously characterized chelators, DFO, H_2PIH, and HDp44mT.

The Ability of the Chelators to Directly Remove ^{59}Fe from Transferrin. To examine the efficacy of the chelators at directly removing ^{59}Fe from the Fe-binding sites of $^{59}Fe_2$-Tf, dialysis experiments were performed using an established procedure.[85] Briefly, $^{59}Fe_2$-Tf (0.75 μM) was incubated with each chelator (25 μM) for 3 h at 37 °C, the solution was then placed in a dialysis sack, and the contents dialyzed with constant mixing for 24 h at 4 °C. Dialysate and the sack were separated and radioactivity assessed as described above.

Ascorbate Oxidation Assay. Briefly, ascorbic acid (100 μM) was prepared immediately prior to an experiment and incubated in the presence of Fe^{III} (10 μM; added as $FeCl_3$), a 50-fold molar excess of citrate (500 μM) and the chelator (1−60 μM). Absorbance at 265 nm was measured after 10 and 40 min at room temperature, and the decrease of intensity between these time points calculated.[5−7] The results of these experiments were expressed in terms of iron-binding equivalents (IBE) due to the varying denticity of the chelators examined. For example, the hexadentate EDTA ligand forms a 1:1 Fe:ligand complex, while tridentate ligands (e.g., HApT series, etc.) form 1:2 Fe:ligand complexes. Three IBEs were chosen, 0.1, 1, and 3, to examine the redox activity of these aroylhydrazones. An IBE of 0.1 represents an excess of Fe, where 1 hexadentate or 2 tridentate ligands are in the presence of 10 Fe atoms. An IBE of 1 results in complete filling of the coordination sphere, while an IBE of 3 represents an excess of the ligand, where 3 hexadentate or 6 tridentate ligands are in the presence of 1 Fe atom.

Statistical Analysis. Experimental data were compared using Student's *t*-test. Results were expressed as mean or mean ± SD (number of experiments) and considered to be statistically significant when $p < 0.05$.

Acknowledgment. P.V.B. and D.R.R. acknowledge the award of an ARC Discovery grant (DP0773027). D.R.R. thanks the National Health and Medical Research Council of Australia for grant and fellowship support. D.B.L. and D.S.K. thank the Cancer Institute NSW for fellowship support. We thank L. Ekman and D. Sharp for technical assistance with some of the biological studies reported herein.

Supporting Information Available: Elemental analyses, NMR and IR spectra for all compounds. This material is available free of charge via the Internet at http://pubs.acs.org.

References

(1) Kalinowski, D. S.; Richardson, D. R. The evolution of iron chelators for the treatment of iron overload disease and cancer. *Pharmacol. Rev.* **2005**, *57*, 547–583.
(2) Hershko, C. Control of disease by selective iron depletion: a novel therapeutic strategy utilizing iron chelators. *Baillieres Clin. Haematol.* **1994**, *7*, 965–1000.
(3) Bernhardt, P. V. Coordination chemistry and biology of chelators for the treatment of iron overload disorders. *J. Chem. Soc., Dalton Trans.* **2007**, 3214–3220.

(4) Bernhardt, P. V.; Caldwell, L. M.; Chaston, T. B.; Chin, P.; Richardson, D. R. Cytotoxic iron chelators: characterization of the structure, solution chemistry and redox activity of ligands and iron complexes of the di-2-pyridyl ketone isonicotinoyl hydrazone (HPKIH) analogues. *J. Biol. Inorg. Chem.* **2003**, *8*, 866–880.

(5) Richardson, D. R.; Sharpe, P. C.; Lovejoy, D. B.; Senaratne, D.; Kalinowski, D. S.; Islam, M.; Bernhardt, P. V. Dipyridyl thiosemicarbazone chelators with potent and selective antitumor activity form iron complexes with redox activity. *J. Med. Chem.* **2006**, *49*, 6510–6521.

(6) Kalinowski, D. S.; Sharpe, P. C.; Bernhardt, P. V.; Richardson, D. R. Design, synthesis, and characterization of new iron chelators with antiproliferative activity: Structure−activity relationships of novel thiohydrazone analogues. *J. Med. Chem.* **2007**, *50*, 6212–6225.

(7) Kalinowski, D. S.; Yu, Y.; Sharpe, P. C.; Islam, M.; Liao, Y.-T.; Lovejoy, D. B.; Kumar, N.; Bernhardt, P. V.; Richardson, D. R. Design, synthesis, and characterization of novel iron chelators: Structure−activity relationships of the 2-benzoylpyridine thiosemicarbazone series and their 3-nitrobenzoyl analogues as potent antitumor agents. *J. Med. Chem.* **2007**, *50*, 3716–3729.

(8) Buss, J. L.; Greene, B. T.; Turner, J.; Torti, F. M.; Torti, S. V. Iron chelators in cancer chemotherapy. *Curr. Top. Med. Chem.* **2004**, *4*, 1623–1635.

(9) Torti, S. V.; Torti, F. M.; Whitman, S. P.; Brechbiel, M. W.; Park, G.; Planalp, R. P. Tumor cell cytotoxicity of a novel metal chelator. *Blood* **1998**, *92*, 1384–1389.

(10) Rakba, N.; Loyer, P.; Gilot, D.; Delcros, J. G.; Glaise, D.; Baret, P.; Pierre, J. L.; Brissot, P.; Lescoat, G. Antiproliferative and apoptotic effects of O-Trensox, a new synthetic iron chelator, on differentiated human hepatoma cell lines. *Carcinogenesis* **2000**, *21*, 943–951.

(11) Richardson, D. R. Molecular mechanisms of iron uptake by cells and the use of iron chelators for the treatment of cancer. *Curr. Med. Chem.* **2005**, *12*, 2711–2729.

(12) Nyholm, S.; Mann, G. J.; Johansson, A. G.; Bergeron, R. J.; Graslund, A.; Thelander, L. Role of ribonucleotide reductase in inhibition of mammalian cell growth by potent iron chelators. *J. Biol. Chem.* **1993**, *268*, 26200–26205.

(13) Cooper, C. E.; Lynagh, G. R.; Hoyes, K. P.; Hider, R. C.; Cammack, R.; Porter, J. B. The relationship of intracellular iron chelation to the inhibition and regeneration of human ribonucleotide reductase. *J. Biol. Chem.* **1996**, *271*, 20291–20299.

(14) Kowol, C. R.; Berger, R.; Eichinger, R.; Roller, A.; Jakupec, M. A.; Schmidt, P. P.; Arion, V. B.; Keppler, B. K. Gallium(III) and iron(III) complexes of α-*N*-heterocyclic thiosemicarbazones: Synthesis, characterization, cytotoxicity, and interaction with ribonucleotide reductase. *J. Med. Chem.* **2007**, *50*, 1254–1265.

(15) Richardson, D. R.; Tran, E. H.; Ponka, P. The potential of iron chelators of the pyridoxal isonicotinoyl hydrazone class as effective antiproliferative agents. *Blood* **1995**, *86*, 4295–4306.

(16) Nurtjahja-Tjendraputra, E.; Fu, D.; Phang, J.; Richardson, D. R. Iron chelation regulates cyclin D1 expression via the proteasome: a link to iron deficiency mediated growth suppression. *Blood* **2007**, *109*, 4045–4054.

(17) Fu, D.; Richardson, D. R. Iron chelation and regulation of the cell cycle: Two mechanisms of post-transcriptional regulation of the universal cyclin-dependent kinase inhibitor p21CIP1/WAF1 by iron depletion. *Blood* **2007**, *110*, 752–761.

(18) Le, N. T. V.; Richardson, D. R. Iron chelators with high antiproliferative activity up-regulate the expression of a growth inhibitory and metastasis suppressor gene: a novel link between iron metabolism and proliferation. *Blood* **2004**, *104*, 2967–2975.

(19) Yuan, J.; Lovejoy, D. B.; Richardson, D. R. Novel di-2-pyridyl-derived iron chelators with marked and selective antitumor activity: in vitro and in vivo assessment. *Blood* **2004**, *104*, 1450–1458.

(20) Whitnall, M.; Howard, J.; Ponka, P.; Richardson, D. R. A class of iron chelators with a wide spectrum of potent antitumor activity that overcome resistance to chemotherapeutics. *Proc. Natl. Acad. Sci. U.S.A.* **2006**, *103*, 14901–14906.

(21) Agrawal, K. C.; Sartorelli, A. C. The chemistry and biological activity of α-(*N*)-heterocyclic carboxaldehyde thiosemicarbazones. *Prog. Med. Chem.* **1978**, *15*, 321–356.

(22) West, D. X.; Liberta, A. E.; Padhye, S. B.; Chikate, R. C.; Sonawane, P. B.; Kumbhar, A. S.; Yerande, R. G. Thiosemicarbazone complexes of copper(II): structural and biological studies. *Coord. Chem. Rev.* **1993**, *123*, 49–71.

(23) Liu, M.-C.; Lin, T.-S.; Sartorelli, A. C. Chemical and biological properties of cytotoxic α-(*N*)-heterocyclic carboxaldehyde thiosemicarbazones. *Prog. Med. Chem.* **1995**, *32*, 1–35.

(24) Casas, J. S.; Garcia-Tasende, M. S.; Sordo, J. Main group metal complexes of semicarbazones and thiosemicarbazones. A structural review. *Coord. Chem. Rev.* **2000**, *209*, 197–261.

(25) Li, J.; Zheng, L.-M.; King, I.; Doyle, T. W.; Chen, S.-H. Syntheses and antitumor activities of ribonucleotide reductase inhibitors: 3-aminopyridine-2-carboxaldehyde-thiosemicarbazone (3-AP) and its phosphate bearing water-soluble prodrugs. *Front. Biotechnol. Pharm.* **2000**, *1*, 314–335.

(26) Quiroga, A. G.; Navarro Ranninger, C. Contribution to the SAR field of metalated and coordination complexes: studies of the palladium and platinum derivatives with selected thiosemicarbazones as antitumoral drugs. *Coord. Chem. Rev.* **2004**, *248*, 119–133.

(27) Greenbaum, D. C.; Mackey, Z.; Hansell, E.; Doyle, P.; Gut, J.; Caffrey, C. R.; Lehrman, J.; Rosenthal, P. J.; McKerrow, J. H.; Chibale, K. Synthesis and structure−activity relationships of parasiticidal thiosemicarbazone cysteine protease inhibitors against *Plasmodium falciparum*, *Trypanosoma brucei*, and *Trypanosoma cruzi*. *J. Med. Chem.* **2004**, *47*, 3212–3219.

(28) Walcourt, A.; Loyevsky, M.; Lovejoy, D. B.; Gordeuk, V. R.; Richardson, D. R. Novel aroylhydrazone and thiosemicarbazone iron chelators with antimalarial activity against chloroquine-resistant and -sensitive parasites. *Int. J. Biochem. Cell Biol.* **2004**, *36*, 401–407.

(29) Biot, C.; Pradines, B.; Sergeant, M.-H.; Gut, J.; Rosenthal, P. J.; Chibale, K. Design, synthesis, and antimalarial activity of structural chimeras of thiosemicarbazone and ferroquine analogs. *Bioorg. Med. Chem. Lett.* **2007**, *17*, 6434–6438.

(30) Kovala-Demertzi, D.; Demertzis, M. A.; Miller, J. R.; Papadopoulou, C.; Dodorou, C.; Filousis, G. Platinum(II) complexes with 2-acetylpyridine thiosemicarbazone. Synthesis, crystal structure, spectral properties, antimicrobial and antitumour activity. *J. Inorg. Biochem.* **2001**, *86*, 555–563.

(31) Kasuga, N. C.; Sekino, K.; Ishikawa, M.; Honda, A.; Yokoyama, M.; Nakano, S.; Shimada, N.; Koumo, C.; Nomiya, K. Synthesis, structural characterization and antimicrobial activities of 12 zinc(II) complexes with four thiosemicarbazone and two semicarbazone ligands. *J. Inorg. Biochem.* **2003**, *96*, 298–310.

(32) Kasuga, N. C.; Onodera, K.; Nakano, S.; Hayashi, K.; Nomiya, K. Syntheses, crystal structures and antimicrobial activities of 6-coordinate antimony(III) complexes with tridentate 2-acetylpyridine thiosemicarbazone, bis(thiosemicarbazone) and semicarbazone ligands. *J. Inorg. Biochem.* **2006**, *100*, 1176–1186.

(33) de Aquino, T. M.; Liesen, A. P.; da Silva, R. E. A.; Lima, V. T.; Carvalho, C. S.; de Faria, A. R.; de Araujo, J. M.; de Lima, J. G.; Alves, A. J.; de Melo, E. J. T.; Goes, A. J. S. Synthesis, anti-*Toxoplasma gondii* and antimicrobial activities of benzaldehyde 4-phenyl-3-thiosemicarbazones and 2-[(phenylmethylene)hydrazono]-4-oxo-3-phenyl-5-thiazolidineacetic acids. *Bioorg. Med. Chem.* **2008**, *16*, 446–456.

(34) Kannan, S.; Sivagamasundari, M.; Ramesh, R.; Liu, Y. Ruthenium(II) carbonyl complexes of dehydroacetic acid thiosemicarbazone: synthesis, structure, light emission and biological activity. *J. Organomet. Chem.* **2008**, *693*, 2251–2257.

(35) Mendes, I. C.; Moreira, J. P.; Ardisson, J. D.; Gouvea dos Santos, R.; da Silva, P. R. O.; Garcia, I.; Castineiras, A.; Beraldo, H. Organotin(IV) complexes of 2-pyridineformamide-derived thiosemicarbazones: antimicrobial and cytotoxic effects. *Eur. J. Med. Chem.* **2008**, *43*, 1454–1461.

(36) Liu, M.-C.; Lin, T.-S.; Penketh, P.; Sartorelli, A. C. Synthesis and antitumor activity of 4- and 5-substituted derivatives of isoquinoline-1-carboxaldehyde thiosemicarbazone. *J. Med. Chem.* **1995**, *38*, 4234–4243.

(37) Baldini, M.; Belicchi-Ferrari, M.; Bisceglie, F.; Dall'Aglio, P. P.; Pelosi, G.; Pinelli, S.; Tarasconi, P. Copper(II) complexes with substituted thiosemicarbazones of α-ketoglutaric acid: synthesis, X-ray structures, DNA binding studies, and nuclease and biological activity. *Inorg. Chem.* **2004**, *43*, 7170–7179.

(38) Padhye, S.; Afrasiabi, Z.; Sinn, E.; Fok, J.; Mehta, K.; Rath, N. Antitumor metallothiosemicarbazonates: structure and antitumor activity of palladium complex of phenanthrenequinone thiosemicarbazone. *Inorg. Chem.* **2005**, *44*, 1154–1156.

(39) Perez-Rebolledo, A.; Ayala, J. D.; de Lima, G. M.; Marchini, N.; Bombieri, G.; Zani, C. L.; Souza-Fagundes, E. M.; Beraldo, H. Structural studies and cytotoxic activity of *N*(4)-phenyl-2-benzoylpyridine thiosemicarbazone Sn(IV) complexes. *Eur. J. Med. Chem.* **2005**, *40*, 467–472.

(40) Adsule, S.; Barve, V.; Chen, D.; Ahmed, F.; Dou, Q. P.; Padhye, S.; Sarkar, F. H. Novel Schiff base copper complexes of quinoline-2 carboxaldehyde as proteasome inhibitors in human prostate cancer cells. *J. Med. Chem.* **2006**, *49*, 7242–7246.

(41) Barker, C. A.; Burgan, W. E.; Carter, D. J.; Cerna, D.; Gius, D.; Hollingshead, M. G.; Camphausen, K.; Tofilon, P. J. In vitro and in vivo radiosensitization induced by the ribonucleotide reductase inhibitor triapine (3-aminopyridine-2-carboxaldehyde-thiosemicarbazone). *Clin. Cancer Res.* **2006**, *12*, 2912–2918.

(42) Hu, W.-X.; Zhou, W.; Xia, C.-N.; Wen, X. Synthesis and anticancer activity of thiosemicarbazones. *Bioorg. Med. Chem. Lett.* **2006**, *16*, 2213–2218.

(43) Kovala-Demertzi, D.; Yadav, P. N.; Wiecek, J.; Skoulika, S.; Varadinova, T.; Demertzis, M. A. Zinc(II) complexes derived from pyridine-2-carbaldehyde thiosemicarbazone and (1*E*)-1-pyridin-2-ylethan-1-one thiosemicarbazone. Synthesis, crystal structures and antiproliferative activity of zinc(II) complexes. *J. Inorg. Biochem.* **2006**, *100*, 1558–1567.

(44) Bisceglie, F.; Baldini, M.; Belicchi-Ferrari, M.; Buluggiu, E.; Careri, M.; Pelosi, G.; Pinelli, S.; Tarasconi, P. Metal complexes of retinoid derivatives with antiproliferative activity: synthesis, characterization and DNA interaction studies. *Eur. J. Med. Chem.* **2007**, *42*, 627–634.

(45) Grguric-Sipka, S.; Kowol, C. R.; Valiahdi, S.-M.; Eichinger, R.; Jakupec, M. A.; Roller, A.; Shova, S.; Arion, V. B.; Keppler, B. K. Ruthenium(II) complexes of thiosemicarbazones: the first water-soluble complex with pH dependent antiproliferative activity. *Eur. J. Inorg. Chem.* **2007**, 2870–2878.

(46) Matesanz, A. I.; Souza, P. Novel cyclopalladated and coordination palladium and platinum complexes derived from α-diphenyl ethanedione bis(thiosemicarbazones): Structural studies and cytotoxic activity against human A2780 and A2780cisR carcinoma cell lines. *J. Inorg. Biochem.* **2007**, *101*, 1354–1361.

(47) Dilovic, I.; Rubcic, M.; Vrdoljak, V.; Pavelic, S. K.; Kralj, M.; Piantanida, I.; Cindric, M. Novel thiosemicarbazone derivatives as potential antitumor agents: synthesis, physicochemical and structural properties, DNA interactions and antiproliferative activity. *Bioorg. Med. Chem.* **2008**, *16*, 5189–5198.

(48) Liu, M. C.; Lin, T. C.; Sartorelli, A. C. Synthesis and antitumor activity of amino derivatives of pyridine-2-carboxaldehyde thiosemicarbazone. *J. Med. Chem.* **1992**, *35*, 3672–3677.

(49) Cory, J. G.; Cory, A. H.; Rappa, G.; Lorico, A.; Liu, M.-C.; Lin, T.-S.; Sartorelli, A. C. Inhibitors of ribonucleotide reductase: comparative effects of amino- and hydroxy-substituted pyridine-2-carboxaldehyde thiosemicarbazones. *Biochem. Pharmacol.* **1994**, *48*, 335–344.

(50) Feun, L.; Modiano, M.; Lee, K.; Mao, J.; Marini, A.; Savaraj, N.; Plezia, P.; Almassian, B.; Colacino, E.; Fischer, J.; MacDonald, S. Phase I and pharmacokinetic study of 3-aminopyridine-2-carboxaldehyde thiosemicarbazone (3-AP) using a single intravenous dose schedule. *Cancer Chemother. Pharmacol.* **2002**, *50*, 223–229.

(51) Wadler, S.; Makower, D.; Clairmont, C.; Lambert, P.; Fehn, K.; Sznol, M. Phase I and pharmacokinetic study of the ribonucleotide reductase inhibitor, 3-aminopyridine-2-carboxaldehyde thiosemicarbazone, administered by 96 h intravenous continuous infusion. *J. Clin. Oncol.* **2004**, *22*, 1553–1563.

(52) Mackenzie, M. J.; Saltman, D.; Hirte, H.; Low, J.; Johnson, C.; Pond, G.; Moore, M. J. A Phase II study of 3-aminopyridine-2-carboxaldehyde thiosemicarbazone (3-AP) and gemcitabine in advanced pancreatic carcinoma. A trial of the Princess Margaret Hospital Phase II consortium. *Invest. New Drugs* **2007**, *25*, 553–558.

(53) Attia, S.; Kolesar, J.; Mahoney, M. R.; Pitot, H. C.; Laheru, D.; Heun, J.; Huang, W.; Eickhoff, J.; Erlichman, C.; Holen, K. D. A phase 2 consortium (P2C) trial of 3-aminopyridine-2-carboxaldehyde thiosemicarbazone (3-AP) for advanced adenocarcinoma of the pancreas. *Invest. New Drugs* **2008**, *26*, 369–379.

(54) Ma, B.; Goh, B. C.; Tan, E. H.; Lam, K. C.; Soo, R.; Leong, S. S.; Wang, L. Z.; Mo, F.; Chan, A. T. C.; Zee, B.; Mok, T. A. multicenter phase II trial of 3-aminopyridine-2-carboxaldehyde thiosemicarbazone (3-AP, Triapine) and gemcitabine in advanced non-small-cell lung cancer with pharmacokinetic evaluation using peripheral blood mononuclear cells. *Invest. New Drugs* **2008**, *26*, 169–173.

(55) Finch, R. A.; Liu, M.; Grill, S. P.; Rose, W. C.; Loomis, R.; Vasquez, K. M.; Cheng, Y.; Sartorelli, A. C. Triapine (3-aminopyridine-2-carboxaldehyde-thiosemicarbazone): a potent inhibitor of ribonucleotide reductase activity with broad spectrum antitumor activity. *Biochem. Pharmacol.* **2000**, *59*, 983–991.

(56) Kumbhar, A.; Sonawane, P.; Padhye, S.; West, D. X.; Butcher, R. J. Structure of antitumor agents 2-acetylpyridinethiosemicarbazone hemihydrate and 2-acetylpyridinethiosemicarbazone hydrochloride. *J. Chem. Crystallogr.* **1997**, *27*, 533–539.

(57) Bermejo, E.; Carballo, R.; Castineiras, A.; Dominguez, R.; Liberta, A. E.; Maichle-Mossmer, C.; Salberg, M. M.; West, D. X. Synthesis, structural characteristics, and biological activities of complexes of Zn(II), Cd(II), Hg(II), Pd(II), and Pt(II) with 2-acetylpyridine-4-methylthiosemicarbazone. *Eur. J. Inorg. Chem.* **1999**, *96*, 5–973.

(58) West, D. X.; Bain, G. A.; Butcher, R. J.; Valdes-Martinex, J.; Toscano, R. A.; Hernandez-Ortega, S.; Jasinsky, J. P.; Li, Y.; Pozdniakiv, R. Y. Structural studies of three isomeric forms of heterocyclic *N*(4)-substituted thiosemicarbazones and two nickel(II) complexes. *Polyhedron* **1996**, *15*, 665–674.

(59) Bermejo, E.; Castineiras, A.; Dominguez, R.; Carballo, R.; Maichle-Mossmer, C.; Strahle, J.; West, D. X. Preparation, structural characterization, and antifungal activities of complexes of group 12 metals with 2-acetylpyridine- and 2-acetylpyridine-*N*-oxide-4*N*-phenylthiosemicarbazones. *Z. Anorg. Allg. Chem.* **1999**, *625*, 961–968.

(60) Kowol, C. R.; Eichinger, R.; Jakupec, M. A.; Galanski, M.; Arion, V. B.; Keppler, B. K. Effect of metal ion complexation and chalcogen donor identity on the antiproliferative activity of 2-acetylpyridine *N*,*N*-dimethyl(chalcogen)semicarbazones. *J. Inorg. Biochem.* **2007**, *101*, 1946–1957.

(61) West, D. X.; Scovill, J. P.; Silverton, J. V.; Bavoso, A. Nickel(II) complexes of a thiosemicarbazone prepared from 2-acetylpyridine. *Transition Met. Chem.* **1986**, *11*, 123–131.

(62) West, D. X.; Billeh, I. S.; Bain, G. A.; Valdes-Martinez, J.; Ebert, K. H.; Hernandez-Ortega, S. Metal complexes of 2-acetylpyridine *N*(4)-dihexyl- and *N*(4)-dicyclohexylthiosemicarbazones. *Transition Met. Chem.* **1996**, *21*, 573–582.

(63) Nomiya, K.; Sekino, K.; Ishikawa, M.; Honda, A.; Yokoyama, M.; Chikaraishi Kasuga, N.; Yokoyama, H.; Nakano, S.; Onodera, K. Syntheses, crystal structures and antimicrobial activities of monomeric 8-coordinate, and dimeric and monomeric 7-coordinate bismuth(III) complexes with tridentate and pentadentate thiosemicarbazones and pentadentate semicarbazone ligands. *J. Inorg. Biochem.* **2004**, *98*, 601–615.

(64) Usman, A.; Razak, I. A.; Chantrapromma, S.; Fun, H. K.; Philip, V.; Sreekanth, A.; Prathapachandra Kurup, M. R. Di-2-pyridyl ketone *N*4,*N*4-(butane-1,4-diyl)thiosemicarbazone. *Acta Crystallogr., Sect. C: Cryst. Struct. Commun.* **2002**, *C58*, o652−o654.

(65) Sreekanth, A.; Kurup, M. R. P. Synthesis, EPR and Mossbauer spectral studies of new iron(III) complexes with 2-benzoylpyridine-*N*(4),*N*(4)-(butane-1,4-diyl) thiosemicarbazone (HBpypTsc): X-ray structure of $[Fe(BpypTsc)_2]FeCl_4 \cdot 2H_2O$ and the free ligand. *Polyhedron* **2004**, *23*, 969–978.

(66) Ketcham, K. A.; Swearingen, J. K.; Castineiras, A.; Garcia, I.; Bermejo, E.; West, D. X. Iron(III), cobalt(II, III), copper(II) and zinc(II) complexes of 2-pyridineformamide 3-piperidylthiosemicarbazone. *Polyhedron* **2001**, *20*, 3265–3273.

(67) Bermejo, E.; Castifieiras, A.; Fostiak, L. M.; Garcia, I.; Llamas-Saiz, A. L.; Swearingen, J. K.; West, D. X. Synthesis; characterization and molecular structure of 2-pyridylformamide *N*(4)-dimethylthiosemicarbazone and some five-coordinated zinc(II) and cadmium(II) complexes. *Z. Naturforsch., B: Chem. Sci.* **2001**, *56*, 1297–1305.

(68) Richardson, D. R.; Bernhardt, P. V. Crystal and molecular structure of 2-hydroxy-1-naphthaldehyde isonicotinoyl hydrazone (NIH) and its iron(III) complex: an iron chelator with antitumor activity. *J. Biol. Inorg. Chem.* **1999**, *4*, 266–273.

(69) Murphy, T. B.; Johnson, D. K.; Rose, N. J.; Aruffo, A.; Schomaker, V. Structural studies of iron(III) complexes of the new iron-binding drug, pyridoxal isonicotinoyl hydrazone. *Inorg. Chim. Acta* **1982**, *66*, L67−L68.

(70) Avramovici-Grisaru, S.; Sarel, S.; Cohen, S.; Bauminger, R. E. The synthesis, crystal and molecular-structure, and oxidation-state of iron complex from pyridoxal isonicotinoyl hydrazone and ferrous sulfate. *Israel J. Chem.* **1985**, *25*, 288–292.

(71) Bernhardt, P. V.; Wilson, G. J.; Sharpe, P. C.; Kalinowski, D. S.; Richardson, D. R. Tuning the antiproliferative activity of biologically active iron chelators: characterization of the coordination chemistry and biological efficacy of 2-acetylpyridine and 2-benzoylpyridine hydrazone ligands. *J. Biol. Inorg. Chem.* **2008**, *13*, 107–119.

(72) Dunford, H. B. Oxidations of iron(II)/(III) by hydrogen peroxide: from aquo to enzyme. *Coord. Chem. Rev.* **2002**, *233*−*234*, 311–318.

(73) Chaston, T. B.; Richardson, D. R. Redox chemistry and DNA interactions of the 2-pyridyl-carboxaldehyde isonicotinoyl hydrazone class of iron chelators: implications for toxicity in the treatment of iron overload disease. *J. Biol. Inorg. Chem.* **2003**, *8*, 427–438.

(74) Chaston, T.; Lovejoy, D.; Watts, R. N.; Richardson, D. R. Examination of the antiproliferative activity of iron chelators: multiple cellular targets and the different mechanism of action of Triapine compared to Desferrioxamine and the potent PIH analogue 311. *Clin. Cancer Res.* **2003**, *9*, 402–414.

(75) Ledru, S.; Boujtita, M. Electrocatalytic oxidation of ascorbate by heme-FeIII/heme-FeII redox couple of the HRP and its effect on the electrochemical behavior of an L-lactate biosensor. *Bioelectrochemistry* **2004**, *64*, 71–78.

(76) Ponka, P.; Schulman, H. M. Acquisition of iron from transferrin regulates reticulocyte heme synthesis. *J. Biol. Chem.* **1985**, *260*, 14717–14721.

(77) Ponka, P.; Schulman, H. M.; Wilczynska, A. Ferric pyridoxal isonicotinoyl hydrazone can provide iron for heme synthesis in reticulocytes. *Biochim. Biophys. Acta* **1982**, *718*, 151–156.

(78) Bernhardt, P. V.; Mattsson, J.; Richardson, D. R. Complexes of cytotoxic chelators from the dipyridyl ketone isonicotinoyl hydrazone (HPKIH) analogues. *Inorg. Chem.* **2006**, *45*, 752–760.

(79) Bernhardt, P. V.; Sharpe, P. C.; Islam, M.; Lovejoy, D. B.; Kalinowski, D. S.; Richardson, D. R. Iron chelators of the dipyridylketone thiosemicarbazone class: precomplexation and transmetalation effects on anticancer activity. *J. Med. Chem.* **2009**, *52*, 407–415.

(80) Richardson, D. R.; Ponka, P. The iron metabolism of the human neuroblastoma cell. Lack of relationship between the efficacy of iron chelation and the inhibition of DNA synthesis. *J. Lab. Clin. Med.* **1994**, *124*, 660–671.

(81) Richardson, D. R.; Milnes, K. The potential of iron chelators of the pyridoxal isonicotinoyl hydrazone class as effective antiproliferative agents II. The mechanism of action of ligands derived from salicylaldehyde benzoyl hydrazone and 2-hydroxy-1-naphthylaldehyde benzoyl hydrazone. *Blood* **1997**, *89*, 3025–3038.

(82) Darnell, G.; Richardson, D. R. The potential of iron chelators of the pyridoxal isonicotinoyl hydrazone class as effective antiproliferative agents III: The effect of the ligands on molecular targets involved in proliferation. *Blood* **1999**, *94*, 781–792.

(83) Baker, E.; Richardson, D. R.; Gross, S.; Ponka, P. Evaluation of the iron chelation potential of hydrazones of pyridoxal, salicylaldehyde and 2-hydroxy-1-naphthylaldehyde using the hepatocyte in culture. *Hepatology* **1992**, *15*, 492–501.

(84) Kontoghiorghes, G. J.; Evans, R. W. Site specificity of iron removal from transferrin by alpha-ketohydroxypyridine chelators. *FEBS Lett.* **1985**, *189*, 141–144.

(85) Bernhardt, P. V.; Chin, P.; Sharpe, P. C.; Wang, J.-Y. C.; Richardson, D. R. Novel diaroylhydrazine ligands as iron chelators: coordination chemistry and biological activity. *J. Biol. Inorg. Chem.* **2005**, *10*, 761–777.

(86) Sheldrick, G. M. *SHELX97. Programs for Crystal Structure Analysis*, release 97-2; University of Göttingen, Göttingen, Germany, 1998.

(87) Farrugia, L. J. ORTEP-3 for windows—a version of ORTEP-III with a graphical user interface (GUI). *J. Appl. Crystallogr.* **1997**, *30*, 565.

(88) Richardson, D. R.; Baker, E. The uptake of iron and transferrin by the human malignant melanoma cell. *Biochim. Biophys. Acta* **1990**, *1053*, 1–12.

(89) Richardson, D.; Baker, E. Two mechanisms of iron uptake from transferrin by melanoma cells. The effect of desferrioxamine and ferric ammonium citrate. *J. Biol. Chem.* **1992**, *267*, 13972–13979.

JM801585U